

# Hysteretic model of the grand piano hammer felt

Anatoli Stulov

Department of Mechanics and Applied Mathematics, Institute of Cybernetics, Akadeemia tee 21, Tallinn, Estonia EE0026

(Received 26 April 1994; accepted for publication 9 December 1994)

The experimental relationships of dynamic force versus grand piano hammer felt deformation show the significant influence of hysteresis characteristics. To explain this phenomenon, a new mathematical model of the hammer felt is proposed. In this model the hammer felt is considered as a nonlinear history-dependent (hysteretic) material with an exponential kernel function. The numerical simulation of interaction of the hammer with a fixed target was used to identify the nonlinear and hysteresis parameters of the felt, and good agreement with experiments was achieved. Also, this model is used here for the analysis of interaction of the hammer with a real grand piano string.

PACS numbers: 43.75.Mn, 43.40.Cw

## LIST OF SYMBOLS

$d$	string diameter	$Q(t)$	acting force
$E_0$	initial hammer energy	$R(t)$	relaxation function
$\epsilon$	hysteresis constant	$T$	string tension
$f$	note frequency	$t$	time
$F_0$	felt stiffness constant	$t_0$	contact time
$F(U)$	force exerted by hammer	$\tau_0$	relaxation constant
$g(y)$	nonlinear force shape function	$\tau=t/\tau_0$	nondimensional time
$L$	string length	$V$	initial hammer speed
$l$	distance of hammer from nearest string end	$Y$	Young's modulus
$m$	hammer mass	$Y_0$	instantaneous Young's modulus
$\mu$	linear mass density of string	$U(t)$	hammer felt compression
$M = \mu L/2$	half of string mass	$W(t)$	string displacement
$p$	stiffness nonlinearity exponent	$w(\tau) = W/d$	nondimensional string displacement
$q = l(L-l)/LT$	string constant	$y(\tau) = U/d$	nondimensional hammer felt compression

## INTRODUCTION

The sound of the grand piano depends mostly on the detailed motion of strings excited by the impact of the hammers. It depends also on the soundboard, of course, but insofar as the soundboard impedance is very much larger than the string impedance, these two problems are separable. So, the creation of good theoretical models of the hammer felt and the hammer-string interaction are important problems for determining the sound produced by a piano.

The dynamics of the hammer-string interaction is one aspect of piano physics that has been the subject of considerable research, beginning with von Helmholtz.<sup>1</sup> Many authors have tried to understand the results of the experimental measurements of the hammer-string interaction and their correspondence to the theoretical models.

In the first model developed by Kaufmann<sup>2</sup> the hammer was assumed absolutely rigid. In other words, this model deals with a point-mass hammer and with a string of limited length. Although this model is far from being realistic, it was used for more than 60 years because of its simplicity.

Hall,<sup>3</sup> in his historical review, commented on the works of many authors, describing the experimental results of felt

deformation under the force acting due to the string. Fletcher and Rossing<sup>4</sup> in their recent review also discussed this problem rather thoroughly. Some special cases of various hammers were considered by Hall.<sup>3,5</sup>

More explicit information about properties of the hammer felt was presented by Suzuki and Nakamura.<sup>6</sup> They reviewed the results of measurements of dynamical hammer-string interaction. These data were obtained experimentally by Yanagisawa, Nakamura and Aiko,<sup>7</sup> and by Yanagisawa and Nakamura.<sup>8,9</sup> Three types of hammers—soft, medium, and hard—acting on various strings were considered in their experiments. These experiments show that:

- (i) Force-compression characteristics of the hammer felt are essentially nonlinear.
- (ii) The slope of the dynamic force-compression characteristics is strongly dependent on the velocity of the hammer.
- (iii) The relationships of dynamic force versus felt deformation show the significant influence of hysteresis characteristics, so the loading and unloading of the felt are not alike.

All of these items are very important and they must be

taken into account in the creation of any realistic hammer felt model. None of the earlier hammer felt models can describe the experimentally observed hysteretic process of loading and unloading of the felt due to the hammer-string interaction.

The present paper is an attempt to construct such a nonlinear hysteretic hammer felt model that would be in a good agreement with experimental data for any rates of loading of the hammer felt. The experiments provided by Yanagisawa and Nakamura<sup>8</sup> are the basis for the testing of the felt model that is proposed in this article. The interaction of such hammer felt with the real grand piano string is presented here only to the extent of illustrating the application of the new model of the hammer felt.

## I. FELT STIFFNESS PROPERTIES

The timbre of sound produced by a piano string is strongly determined by the contact time between the hammer and the string. In turn, this time depends on the stiffness of the hammer felt and hammer velocity. Therefore the contact time between the hammer and the string is decreased by a strong attack and the number of harmonics in the spectrum is increased. Thus the timbre of sound in the lower and the middle range of the instrument is appreciably dependent on the average variation of the felt stiffness.

An excellent feature of a good grand piano is the possibility to obtain more “brilliant” or “transparent” timbre of sound when playing *fortissimo*, and on the contrary “smooth” timbre when playing *pianissimo*. Such a timbre can be achieved from properly designed hammer felt stiffness for various possible velocities of the hammer.

One of the first nonlinear models of the hammer felt was made by Ghosh,<sup>10</sup> who considered the felt as a material obeying the power law

$$F = AU^p, \quad A = \text{const.} \quad (1)$$

Using this model Hall and Askenfelt<sup>11</sup> measured the values of  $p$  for 16 real samples of hammers. For the load force  $F$  ranging from 0.55 to 35 N these hammers had  $p$  between 1.5 and 3.5 with no definite trend of  $p$  from bass to treble. One hammer was exceptional, with  $p=5.0$ .

According to Hertz's Law the force acting on two connected locally Hookean bodies gives  $p=1.5$ . The values of  $p$  different from 1.5 indicate the non-Hooke or the nonlocal felt properties. As discussed in Ref. 11, the value of  $p=1$  gives a simple linear system but it has an unmusical property because both loud and soft notes are amplified equally. In the author's opinion, the most suitable values of  $p$  for a good grand piano are  $2 < p < 3$ , while  $p \geq 3$  gives too much contrast in tone when playing *fortissimo* versus *pianissimo*.

Hall<sup>12</sup> used this nonlinear power-law model of the felt for the modeling of the hammer-string interaction and obtained a better agreement with earlier data than using his previous calculations based on a completely linear model.

The interaction of the string with a nonlinear hammer felt has been studied by Suzuki.<sup>13</sup> The force-compression relationship of the hammer felt was approximated in his article in the form

$$F = K_1U^2 + K_2U^3 + K_3U^4, \quad (2)$$

with the constant stiffness coefficients  $K_1$ ,  $K_2$ , and  $K_3$ . It seems this model is not satisfactory, because the first coefficient  $K_1$  is negative and so for small felt deformations the force has a negative value, too. This is impossible, since the hammer does not pull the string.

Both the power-law and polynomial models are often used for the mathematical simulation of the hammer-string interaction. But the process of the felt deformation described by Eqs. (1) and (2) is nonhysteretic. The loading and unloading of the felt in such models occurs in the same way.

Boutillon<sup>14</sup> has made an attempt to explain the clearly nonlinear hysteretic character of the hammer-string interaction using the model of the point hammer mass and a nonlinear hysteretic spring that describes the action of the felt. He uses the same power law (1) for description of the force acting on the felt, but with various constant values of the exponent  $p$  for the increasing and decreasing part of the spring characteristic. According to this nonanalytical model, the felt deformation tends to zero with the unloading of the felt. To avoid this behavior, the partial hysteretic characteristics due to the waves traveling back and forth along the string were included in this model. The agreement of the model with the experimental measurements obtained by author was rather good. However, other experiments<sup>6-9</sup> show that the felt is still deformed after the force is removed even in the absence of waves traveling along the string. Also, the value of the exponent  $p$  in this nonanalytical model cannot be a constant, because the slope of the dynamic force-compression characteristics is dependent on the velocity of the hammer. For this reason, even the loading part of the force-compression curve cannot be described by the simple Eq. (1) with a constant value of  $p$  that must be different for the various hammer velocities.

A somewhat more realistic analytical model of the hammer felt that is in agreement with experiments (see Refs. 8 and 9) at all points will be presented in the following section.

## II. HAMMER FELT MODEL

In deriving a dynamical hammer felt model it is necessary to take into consideration both the hysteresis of the force-compression characteristics and their dependence on the hammer speed. These phenomena require that the grand piano hammer felt possess history-dependent properties. The mechanical behavior of such materials is usually strongly dependent on parameters such as time, characteristic frequency, and rate of loading. For this reason the stress-strain curves of history-dependent materials are sensitive to these quantities, and the concept of an almost unique curve for a given material does not exist.

In the hammer-string interaction the process of the felt deformation starts with some velocity  $V > 0$ , and we obtain a certain loading curve for the hammer felt. The unloading of the felt begins with velocity  $V = 0$ , and the unloading curve of the felt will not be like the loading curve. Therefore for felt made of history-dependent material the loading-unloading curve has hysteresis characteristics.

TABLE I. Primary parameters of the grand piano hammers and strings.

Quantity	Notes		
	A <sub>0</sub>	A <sub>3</sub>	A <sub>6</sub>
<i>f</i> (Hz)	28	220	1760
<i>L</i> (mm)	2016	777	115
<i>l</i> (mm)	243	91	8.1
<i>d</i> (mm)	4.9	1.075	0.875
<i>T</i> (N)	1629	834	774
<i>μ</i> (g/m)	130.7	7.1	4.7
<i>m</i> (g)	13.0	10.6	8.2

As indicated by Rabotnov,<sup>15</sup> a simple model of material with memory may be obtained by means of replacing constant elastic parameters of solids by time-dependent operators. So for the case of longitudinal one-dimensional deformation of a body with memory, the Young's modulus is now not a constant, but an operator

$$Y(t) = Y_0[1 - R(t)*], \tag{3}$$

where \* denotes the convolution sign.

Suppose that the force exerted by the hammer under the instantaneous loading of the felt is proportional to the Young's modulus of the felt material, and can be described by a nonlinear force shape function of the form

$$F(U) = CYg(U), \tag{4}$$

with some constant coefficient *C*. In this case, using (3) for the arbitrary rate of loading, the hysteretic felt is defined with the aid of the constitutive equation

$$F(U(t)) = F_0[g(U(t)) - R(t)*g(U(t))]. \tag{5}$$

Materials described by this equation for which the exerted force (or the stress) is determined by the history of the compression are "materials with memory."

In principle, *R(t)* is to be established for real media on the basis of experimental data. However, according to well-known general physical consideration (see Ref. 15), some properties of the relaxation function might be assumed for real history-dependent media with almost no restriction of generality.

The relaxation function *R(t)* must be a positive function, which is bounded in the interval  $0 < t < \infty$ , and satisfies the following conditions:

$$\lim_{t \rightarrow 0} \int_0^t R(\xi) d\xi = 0, \tag{6}$$

$$R(t) \rightarrow 0, \text{ if } t \rightarrow \infty, \tag{7}$$

$$0 < \epsilon < 1, \tag{8}$$

where

$$\epsilon = \int_0^\infty R(t) dt. \tag{9}$$

By this assumption rather weak restrictions are laid on the function *R(t)*.

Let us choose a simple form of the relaxation function given by

$$R(t) = (\epsilon/\tau_0) \exp(-t/\tau_0). \tag{10}$$

In Eq. (10) the history-dependent material of the hammer felt is defined with the aid of two hysteresis parameters  $\epsilon$  and  $\tau_0$ . Now, using Eq. (10), Eq. (5) can be written in dimensionless form as

$$F(y(\tau)) = F_0 \left( g(y(\tau)) - \epsilon e^{-\tau} \int_0^\tau e^\xi g(y(\xi)) d\xi \right). \tag{11}$$

This is the governing equation connecting the force *F(y)* exerted by hammer and the felt deformation *y(τ)*. Then we explore the possibility of getting the theoretical results to match the experimental data for real hammers through a proper choice of numerical values of these parameters.

From Eq. (11) we may obtain the form of the force-compression characteristic for very fast felt deformation, when  $\tau \ll 1$ ,

$$F(y) = F_0 g(y), \tag{12}$$

and for very slow deformation, when  $\tau \gg 1$ ,

$$F(y) = F_0(1 - \epsilon)g(y). \tag{13}$$

In each of these cases the unloading of the felt occurs in the same way as the loading.

For the various types of hammers the nonlinear force shape function *g(y)* can be chosen in the power polynomial form or in the form of the usual power-law dependence

$$g(y) = y^p, \tag{14}$$

in order to describe rather well very fast loading of the felt. Finally, the governing equation (11) in connection with the

TABLE II. Numerically determined parameters of the hammers.

Quantity	Hammers									
	A1				A37			A73		
	hard	medium	soft	pliant	hard	medium	soft	hard	medium	soft
<i>F</i> <sub>0</sub> (kN)	242.6	200.6	64.7	38.9	9.43	3.58	1.05	10.66	9.31	8.48
<i>p</i>	2.87	2.95	2.80	2.19	3.40	3.30	2.81	3.15	3.12	3.33
<i>τ</i> <sub>0</sub> (μs)	10.5	11.5	17.0	20.0	5.5	7.0	10.0	1.9	2.1	2.0
$\epsilon$	0.947	0.947	0.940	0.936	0.968	0.956	0.938	0.981	0.985	0.985
<i>V</i> (m/s)	1.25	1.31	1.52	1.45	1.25	1.36	1.60	1.35	1.47	1.47
<i>t</i> <sub>0</sub> (ms)	1.37	1.47	1.63	1.32	1.21	1.34	1.52	1.01	1.04	1.09

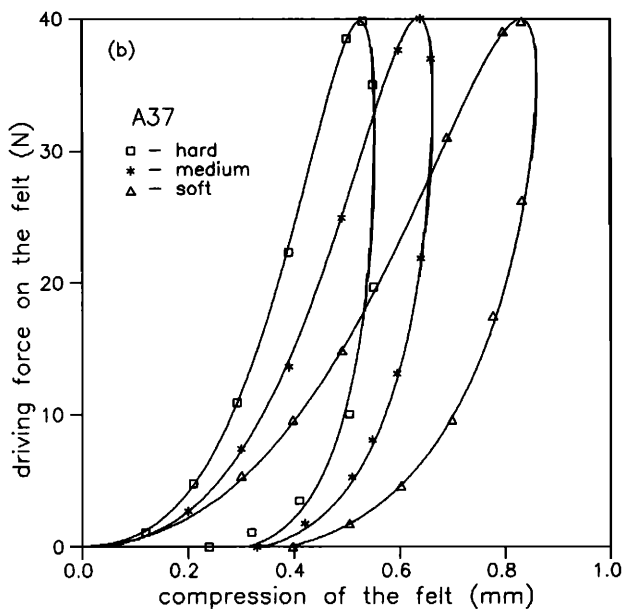
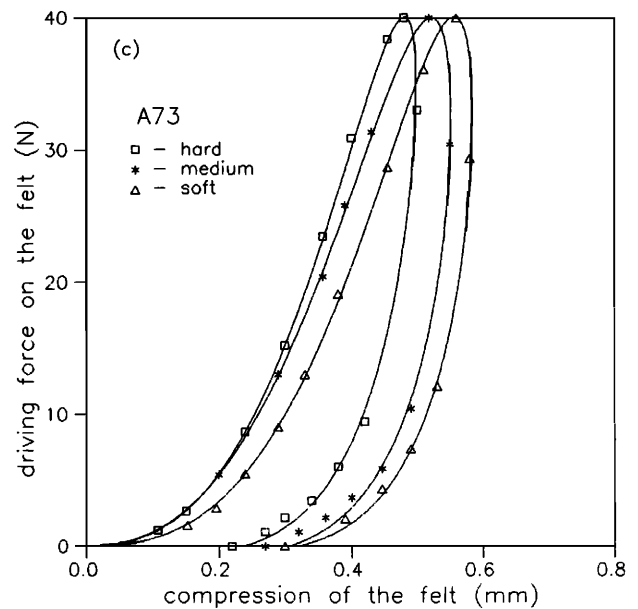
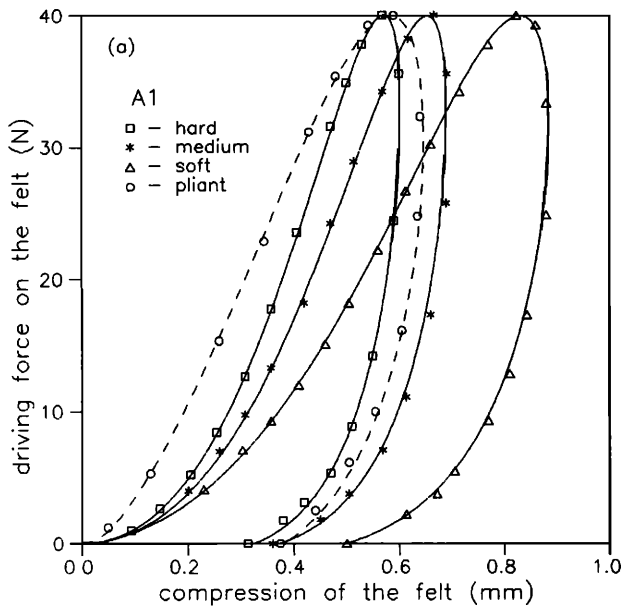


FIG. 1. Force–compression characteristics of the felt for (a) A1 hammer, (b) A37 hammer, and (c) A73 hammer. Squares, asterisks, triangles, and circles denote the experimental data points (Ref. 8). The solid [and one dashed on (a)] lines are the calculated curves for each type of the felt.

nonlinear force shape function in the form (14) is the hysteretic model of the grand piano hammer felt which is proposed in this article.

### III. NUMERICAL SIMULATION OF EXPERIMENT

Comparison with experiment is the way to judge the success of the present model. The experimental data on the dynamical felt deformation obtained in Ref. 8 were chosen for this purpose. In these measurements the hammer struck the piece of string fixed on the force sensor, and the force–compression and stiffness–time relationships for the various types of hammers were obtained.

The mathematical model of this experiment can be described with dimensionless variables by the equation

$$\frac{d^2y}{d\tau^2} = \frac{\tau_0^2}{m\bar{d}} F(y), \quad (15)$$

with the initial conditions

$$y(0) = 0, \quad \frac{dy}{d\tau}(0) = \frac{\tau_0 V}{d}. \quad (16)$$

Here  $F(y)$  is defined by Eqs. (11) and (14).

Equation (15) was solved numerically by a modified Euler's method. In order to obtain that solution, we must know the parameters that describe both the string and the hammer. Unfortunately in Ref. 8 the masses of the hammers are not given. Thus the comparison between the experimental and the theoretical results is not always correct.

Some of the parameters of the hammers and the strings are well known, or they can be measured rather easily. The values of such primary parameters of the grand piano for notes  $A_0$ ,  $A_3$ , and  $A_6$  are displayed in Table I. Here the mass of the hammer is the effective mass, which is measured in the same way as in Ref. 14. All the values in Table I refer only to the particular grand piano ESTONIA that we used.

Initially unknown, the values of the felt parameters were obtained by means of numerical simulation of the model.

The force–compression characteristic  $F(y)$  was numerically calculated from Eq. (15) by assuming initial values of the felt parameters. The model was run again and again, each time with different felt parameter values, until the prediction from the model gave good agreement with the experimental data.

In experiments<sup>8</sup> with the constant maximum value of the driving force on the felt the hard, medium, and soft hammers with numbers A1 (note  $A_0$ ), A37 (note  $A_3$ ), and A73 (note  $A_6$ ) were used. An unusual type of A1 hammer (termed pliant) that differs from all other A1 hammers used in the first series of experiments was investigated for dynamical impact of the string with various initial velocities. The final values of the numerically determined parameters of the felt are displayed in Table II for all the hammers considered.

The comparison of the theoretical model with the experimental data is presented in Fig. 1. The agreement of the results from the hysteretic model with the experimental results of Ref. 8 is rather good. The analysis of parameters presented in Table II show that the felt stiffness constant  $F_0$  and hysteresis constant  $\epsilon$  are diminished, and vice versa the relaxation constant  $\tau_0$  is increased with the softening of the felt for the hammers in the range from A1 to A37. The parameters of the hard, medium, and soft A73 hammer are close to each other, which was expected from Fig. 1(c). The value of  $p$  for any number of hammers has no definite trend from hard to soft. Only for the pliant hammer the value of  $p$  is outstanding. The absence of the trend in the set of calculated values is due to the entirely arbitrary types of hammers chosen for the experiments. So the pair of quite different A1 hammers was used.

It is obvious that the A1 pliant hammer is really exceptional. The values of stiffness and hereditary parameters of this hammer indicate that the pliant hammer is not a hard hammer, as it seems from Fig. 1(a), but most probably, it is very soft. This is clear from Fig. 2(a), where the dynamical force–compression characteristics for the various hammer velocities are shown. With a diminishing of the hammer speed, the slope of the loading part of the curves is decreased. To obtain a better agreement with the experimental data points for a small velocities of hammer, the value of stiffness nonlinearity exponent  $p=2.15$  was chosen (other parameters of the pliant hammer are the same as in Table II). The numerically calculated stiffness–time characteristics of this A1 pliant hammer are shown in Fig. 2(b). They are very similar to those experimentally obtained in Ref. 8.

The numerical calculations are provided here only to demonstrate the quality of the hysteretic model, and not for determination of the exact values of the felt parameters. It is shown that the model can describe the loading and unloading parts of the force–compression curve for suitable values of primary parameters. By using the primary parameter values of the grand piano ESTONIA, which are certainly not the same as those used in the experiments, the numerically calculated hammer velocities differ from velocities in the experiments by less than 20%. Of course, under other initial conditions the calculated values of the felt parameters would be changed, but the form of the force–compression curve can be described by the hysteretic model with any desired accuracy.

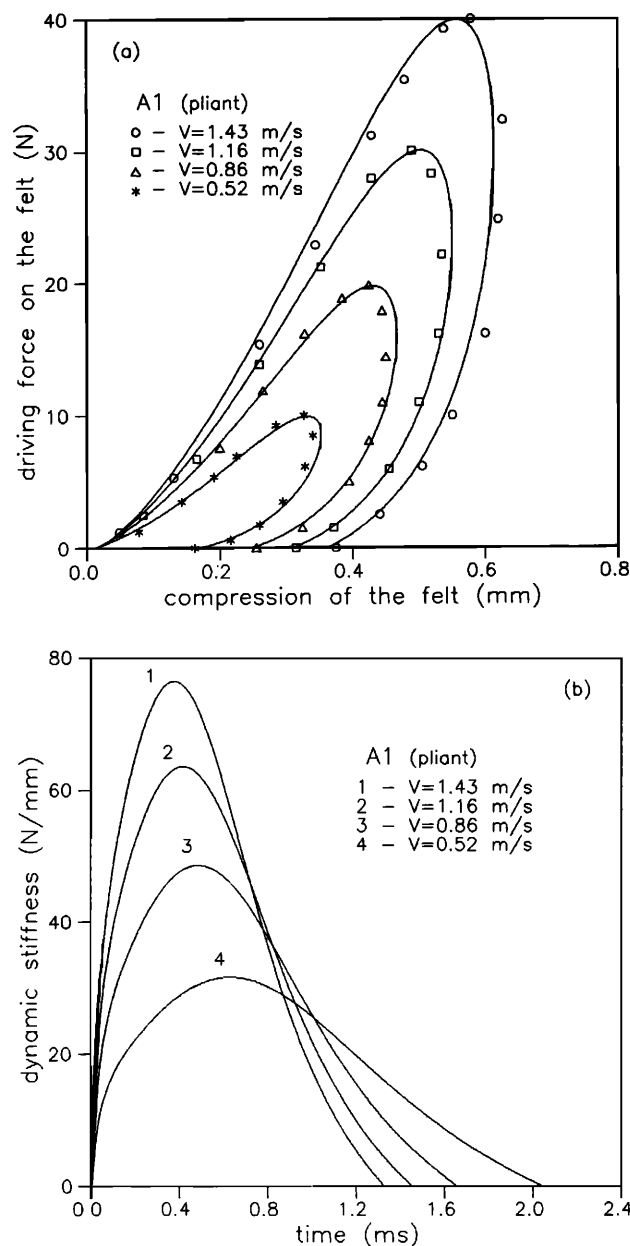


FIG. 2. (a) Force–compression and (b) stiffness–time characteristics of the felt for A1 (pliant) hammer for the various initial hammer velocities. Circles, squares, triangles, and asterisks denote the experimental data points (Ref. 8). The solid lines are the calculated curves.

#### IV. HYSTERETIC MODEL FEATURES

The influence of the hammer speed and of the hysteresis parameters of the felt on the force–compression characteristic is presented in Fig. 3. Figure 3(a) shows the loading and unloading of the felt for various initial hammer velocities. The initial hammer energy in this case is a constant and is equal to 1.8 mJ. The mass of the hammer is not a constant for the various curves, but ranges from 0.001 to 1000 g.

The contact times calculated for each curve are displayed in Table III. For the initial hammer velocity  $V=60$  m/s, the dimensionless contact time is equal to  $t_0/\tau_0=0.37 < 1$ . So as was mentioned above, the loading and unloading of the felt under the fast deformation are close to the limit curve I that is described by Eq. (12). For the

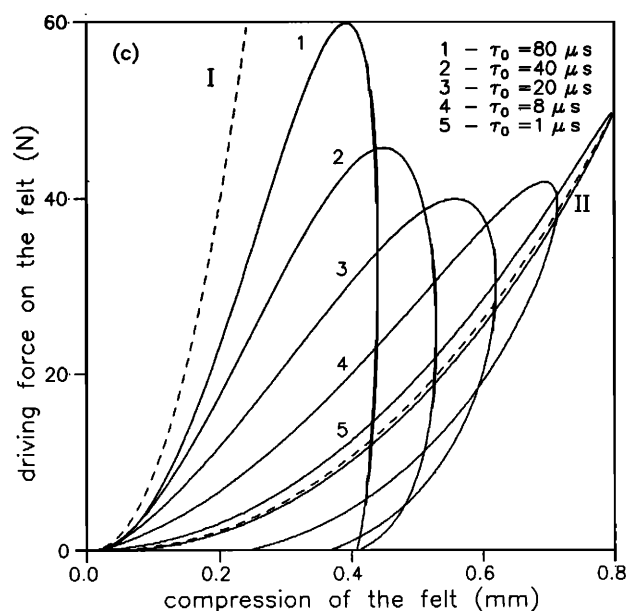
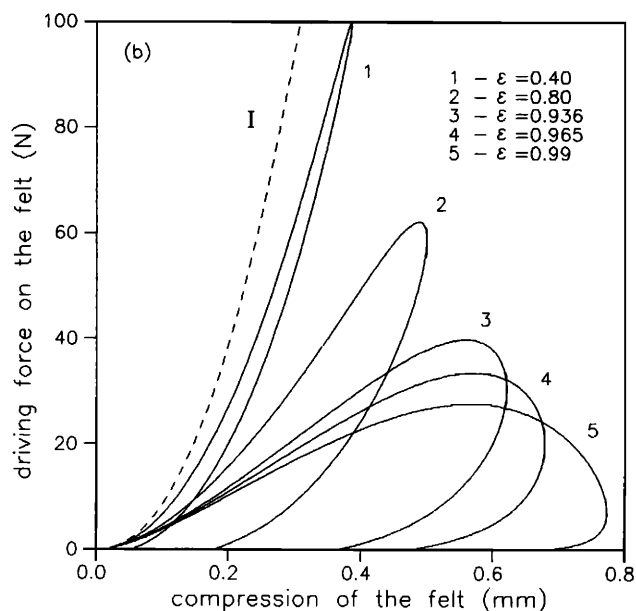
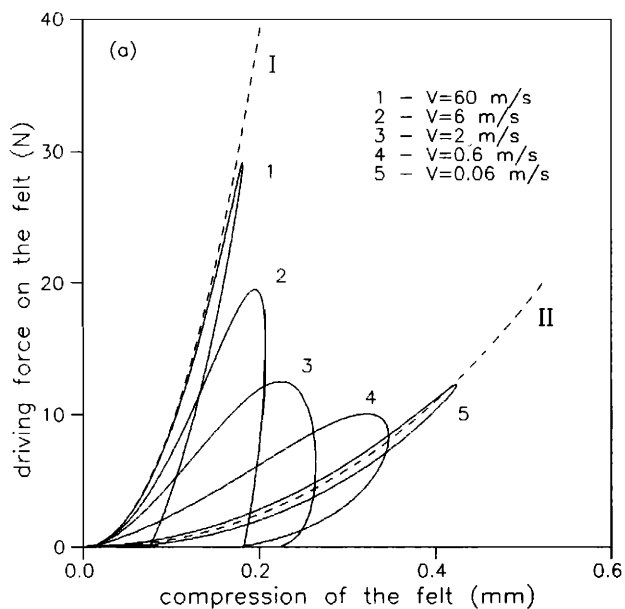


FIG. 3. Force-compression characteristics for A1 (pliant) hammer. (a) Varying the initial hammer speed (initial hammer energy is constant); (b) varying hysteresis constant; (c) varying the relaxation constant of the felt. Dashed lines I and II are limit curves for very fast and very slow felt loading, respectively.

initial hammer velocity  $V=0.06$  m/s, the dimensionless contact time is equal to  $t_0/\tau_0=1000 \gg 1$ . For this slow deformation, the loading and the unloading of the felt are near the limit curve II described by Eq. (13).

Force-compression curves calculated for different values of the hysteresis constant are shown in Fig. 3(b). For the case of  $\epsilon=0$ , the loading and unloading of the felt occur along the limit curve I.

Force-compression curves calculated for different values of the relaxation constant are presented in Fig. 3(c). For

small values of  $\tau_0$  the loading and unloading parts of the curve are close to the limit curve II.

As shown in Table III, contact time increases with an increasing hysteresis constant and with a decreasing relaxation constant. The results of calculations presented in Fig. 3 permit one to study the influence of the felt parameters on the form of the force-compression characteristics. The theoretical hysteretic model of hammer felt provides a means for simulating any necessary force-compression curve.

## V. GRAND PIANO HAMMER-STRING INTERACTION

The hysteretic hammer felt model may also be used for describing an actual hammer-string interaction. In the experiment described in Ref. 8 the string was fixed on the force sensor. The real grand piano string moves under the hammer action.

When the key is pressed down the hammer, in its rotation around the pivot, strikes the string with some velocity  $V$  which is directed upward. The string begins pushing back on

TABLE III. Duration of contact time calculated for the various parameters of A1 (pliant) hammer.

Curve number	Duration of contact (ms)				
	1	2	3	4	5
Fig. 3(a)	0.0074	0.074	0.38	1.76	20.0
Fig. 3(b)	0.74	0.99	1.32	1.52	2.0
Fig. 3(c)	0.71	1.12	1.32	1.46	1.56

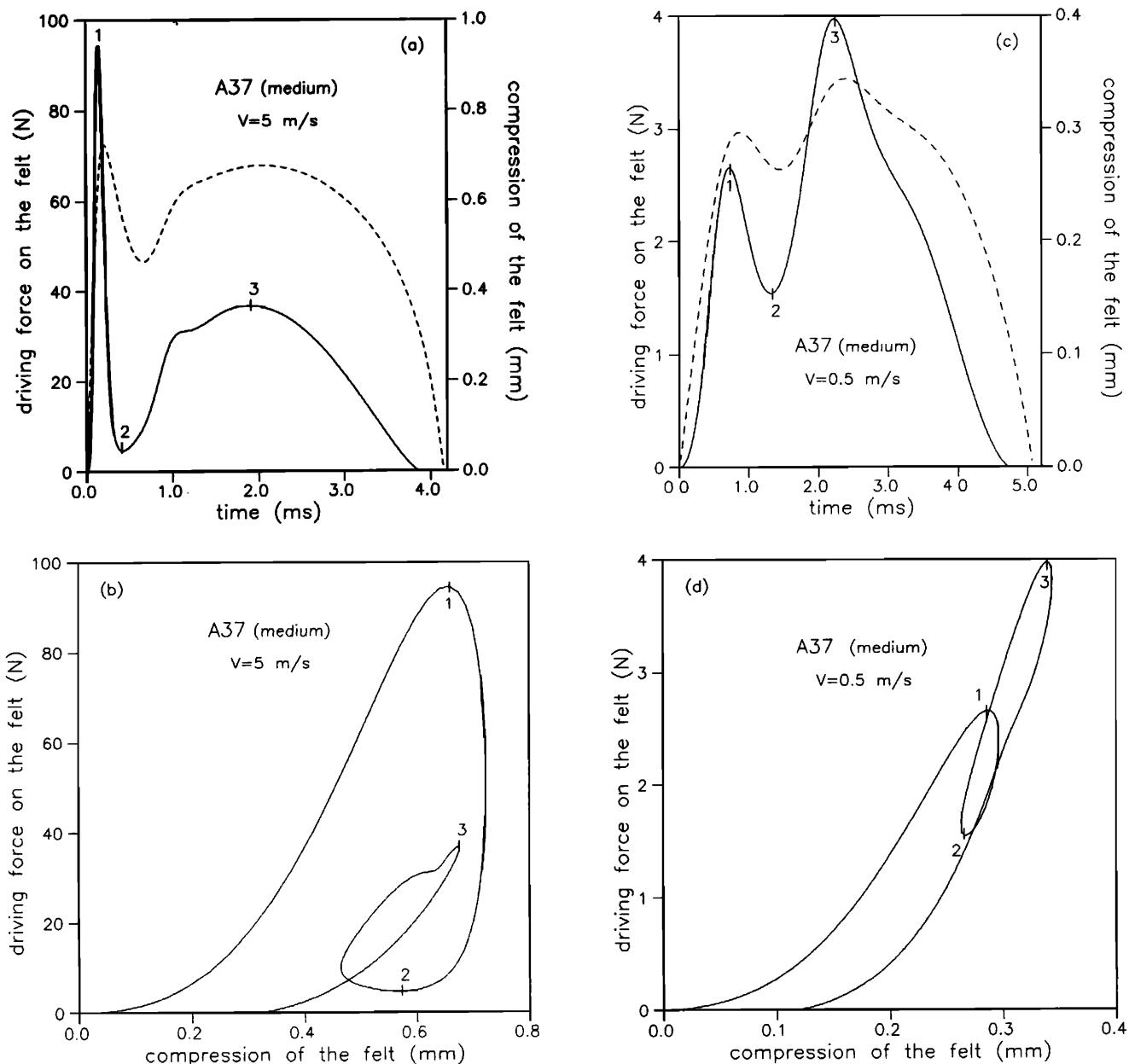


FIG. 4. For A37 (medium) hammer (a), (c) time histories and (b), (d) force–compression characteristics numerically calculated for the real grand piano note  $A_3$ . The initial hammer velocities are  $V=5$  and  $0.5$  m/s. The solid lines on (a) and (c) are the force–time curves, and the dashed lines are the compression–time curves.

the hammer, and at the end of interaction the hammer moves away from the string. The angular displacement during the collision is quite small so that the hammer’s movement is treated as a simple translation.

Consider an idealized model of the string, in which the two portions of the string can be represented as slowly rotating straight segments. This model is true for a slow loading of the string when the hammer–string interaction takes a very long time compared to the natural period of the string vibrations. In all examples presented below, the contact time between the hammer and the string is greater than the period of vibration of the string, and so this model of the string corresponds to the hammer–string interaction in the middle and treble ranges.

According to this simple string model, the displacement

of the string from the equilibrium position is proportional to the force  $Q(t)$  acting on the string:

$$W = qQ. \quad (17)$$

Because only half of the total mass of the string is deflected to the distance  $W$  in this linear model, the motion of the string is defined by the equation

$$M \frac{d^2W}{dt^2} = F - Q. \quad (18)$$

The displacement of the hammer  $Z(t)$  depends on both the felt deformation and the string deflection

$$Z = U + W, \quad (19)$$

and the equation of motion of the hammer is

$$m \frac{d^2 Z}{dt^2} + F = 0. \quad (20)$$

By choosing for a unit length the string diameter, from Eqs. (17)–(20), we obtain a system of equations for description of the hammer–string interaction in nondimensional variables

$$\frac{d^2 w}{d\tau^2} = -\frac{\tau_0^2}{Mq} w + \frac{\tau_0^2}{Md} F(y) = 0, \quad (21)$$

$$\frac{d^2 y}{d\tau^2} = \frac{\tau_0^2}{Mq} w - \frac{\tau_0^2}{Md} \left(1 + \frac{M}{m}\right) F(y) = 0. \quad (22)$$

Here the function  $F(y)$  is also defined by Eqs. (11) and (14). The initial conditions for this system of equations are

$$y(0) = w(0) = \frac{dw}{d\tau}(0) = 0, \quad (23)$$

$$\frac{dy}{d\tau}(0) = \frac{\tau_0 V}{d}. \quad (24)$$

The system of equations (21) and (22) was numerically solved by the modified Euler's method, and the results of the hammer–string interaction are presented in Figs. 4 and 5. All parameters of the hammers and the strings are taken from Tables I and II.

Figure 4 shows the interaction of the A37 medium hammer with one string (of a three-string set) for  $A_3$ .

When the hammer with velocity  $V=5$  m/s [Fig. 4(a)] strikes the string, the driving force on the felt is increased in time from the initial point to point 1, and the string is accelerated. At point 1 the velocity of the string is greater than the velocity of the hammer and the string begins to run away from the hammer, but the contact between the hammer and the string is maintained. Therefore between points 1 and 2 the driving force is decreased, and the felt partly unloads.

After maximum deflection, the string increases its driving force on the hammer as shown between points 2 and 3; this fact is not connected with the exact form of the waves traveling along the string. After point 3, the speed of the hammer is greater than the speed of the string, and the hammer moves away from the string. The hammer loses the contact with the string 3.83 ms after the beginning of interaction. At this time the felt is still partly loaded, and complete unloading of the felt occurs with some velocity due to its history-dependent features. The contact time in this case is approximately equal to the period of vibrations of this string.

A bend on the force–time characteristic between the points 2 and 3 takes place due to the memory of the felt, and its place depends on the rate of the felt loading [compare Fig. 4(c)]. The form of the compression–time curve is similar to the force–time characteristic, but compression is slightly delayed due to relaxation. The force–compression characteristic for this case with corresponding points is shown in Fig. 4(b). If the initial speed of the hammer were greater than 5

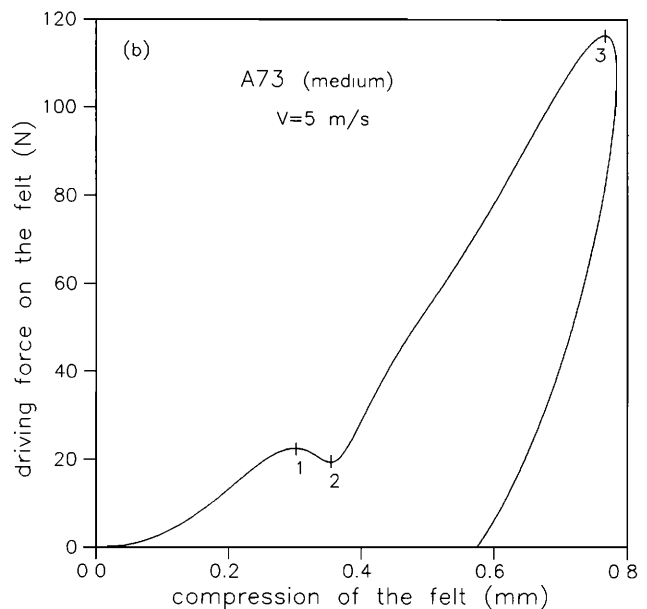
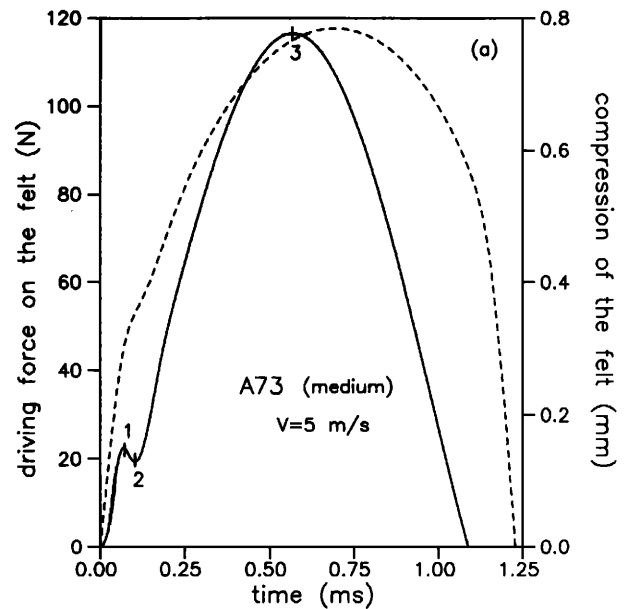


FIG. 5. For A73 (medium) hammer with initial velocity  $V=5$  m/s (a) time histories and (b) force–compression curves numerically calculated for the real grand piano note  $A_6$ . The solid line on (a) is the force–time curve, and the dashed line is the compression–time curve.

m/s, point 2 on the force–time characteristic would be lowered, and the hammer would lose contact with the string in approximately 0.4 ms at the beginning of interaction. In this case we would see a second, repeated strike, when the string catches up with the hammer in reverse motion.

In Fig. 4(c) and (d) similar patterns are presented for a small initial hammer velocity. In this case the maximum value of the driving force on the felt is achieved only at point 3 in the reverse motion of the string. This fact is more noticeable in the treble range as shown in Fig. 5. Here the interaction of the A73 hammer with the string of  $A_6$  is presented. Because the natural vibration frequency of this string is rather high, the string runs away rapidly from the hammer after the initial interaction. So the main compression of the

felt occurs in the contrariwise motion of the hammer and the string at point 3.

The contact time in this case is equal to 1.1 ms, and is twice greater than the period of the string vibrations.

## VI. CONCLUSION

It has been shown that reasonable assumptions about the history-dependent properties of hammer felt provide the basis for a simple mathematical model for investigation of the piano hammer–string interaction. The model of felt with memory permits a description of the felt deformation that is consistent with experiments. The model demonstrated here makes predictions in good agreement with experimental data for various types of piano hammers and for a broad range of hammer velocities.

The numerical simulation of the interaction of a hammer with a fixed target permits the determination of the values of the stiffness and hysteresis parameters of the hammers used in the experiments. The interaction of a hysteretic hammer with a highly idealized string presented in Sec. V is only a first step in the direction of using of this model and the results probably give a correct qualitative indication of the effect of hysteresis for high notes. Further application of this model should include the interaction of the hysteretic hammer with more realistic models of the string in order to get results that come closer to measurements in real pianos.

## ACKNOWLEDGMENTS

I am grateful to Professor Jüri Engelbrecht and Arkadi Berezovsky for many helpful discussions. This research was sponsored by a contract from the Grand Piano Factory in Tallinn, Estonia.

- <sup>1</sup>H. von Helmholtz, *On the Sensations of Tone*, translated by A. J. Ellis (Dover, New York, 1954), pp. 74–80, 380–384.
- <sup>2</sup>W. Kaufmann, *Ann. Phys. (Leipzig)* **54**, 675–712 (1895).
- <sup>3</sup>D. E. Hall, *J. Acoust. Soc. Am.* **81**, 547–555 (1987).
- <sup>4</sup>N. H. Fletcher and T. D. Rossing, *The Physics of Musical Instruments* (Springer-Verlag, New York, 1991), pp. 319–321.
- <sup>5</sup>D. E. Hall, *J. Acoust. Soc. Am.* **81**, 535–546 (1987).
- <sup>6</sup>H. Suzuki and I. Nakamura, *Appl. Acoust.* **30**, 147–205 (1990).
- <sup>7</sup>T. Yanagisawa, K. Nakamura, and H. Aiko, *J. Acoust. Soc. Jpn.* **37**, 627–633 (1981).
- <sup>8</sup>T. Yanagisawa and K. Nakamura, *Trans. Musical Acoust. Techn. Group Meeting Acoust. Soc. Jpn.* **1**, 14–18 (1982).
- <sup>9</sup>T. Yanagisawa and K. Nakamura, *J. Acoust. Soc. Jpn.* **40**, 725–729 (1984).
- <sup>10</sup>M. Ghosh, *Indian J. Phys.* **7**, 365–382 (1932).
- <sup>11</sup>D. E. Hall and A. Askenfelt, *J. Acoust. Soc. Am.* **83**, 1627–1638 (1988).
- <sup>12</sup>D. E. Hall, *J. Acoust. Soc. Am.* **92**, 95–105 (1992).
- <sup>13</sup>H. Suzuki, *J. Acoust. Soc. Am.* **82**, 1145–1151 (1987).
- <sup>14</sup>X. Boutillon, *J. Acoust. Soc. Am.* **83**, 746–754 (1988).
- <sup>15</sup>J. N. Rabotnov, *Elements of Hereditary Mechanics of Solids* (Nauka, Moscow, 1977), pp. 54–60, 97–101.